



# Enhanced Energy Harvesting Using Multilayer Piezoelectric Ceramics

SATYANARAYAN PATEL,<sup>1,2</sup> IN-TAE SEO,<sup>2,3,6</sup> and SAHN NAHM<sup>4,5</sup>

1.—Department of Mechanical Engineering, Malaviya National Institute of Technology Jaipur, Jaipur, Rajasthan 302017, India. 2.—Institute of Materials Science, Technische Universität Darmstadt, FB Nichtmetallische-Anorganische Werkstoffe, Alarich-Weiss-Strasse 2, 64287 Darmstadt, Germany. 3.—MLCC Materials Development Group, Samsung Electro-Mechanics Co., Ltd., 150 Maeyoung-ro, Suwon, Gyeonggi-do, Korea. 4.—Department of Materials Science and Engineering, Korea University, Anam-dong 5-ga, Seongbuk-gu, Seoul 136-701, Korea. 5.—KU-KIST Graduate School of Converging Science and Technology, Korea University, Seoul 136-701, Korea. 6.—e-mail: intae2017.seo@samsung.com

In this work, multi-layer ceramics (MLC) are fabricated for vibrational energy harvesting using 0.5 mol.% CuO added 0.69Pb(Zr<sub>0.47</sub>Ti<sub>0.53</sub>)O<sub>3</sub>-0.31Pb(Zn<sub>0.4</sub>Ni<sub>0.6</sub>)<sub>1/3</sub>Nb<sub>2/3</sub>O<sub>3</sub> (0.5CPZT-PZNN). 0.5CPZT-PZNN has a high transduction coefficient of 20,367 m<sup>2</sup>/N with a high Curie temperature of 300°C. The effect of the number of layers (*n*-layers = 1, 3, 5 and 7) on the active power density is systematically investigated. MLC-based piezoelectric energy harvesting (PEH) can increase the active power output by approximately 2.5 times as compared to bulk PEH (*n* = 1). For the bulk ceramic, PEH active power density is found to be 21 mW/cm<sup>3</sup>, whereas maximum active power density is obtained for *n* = 5 (49.7 mW/cm<sup>3</sup>). However, upon increasing layers (*n* = 7), active power density is decreased due to high capacitance. The result shows that the MLC-based PEH can increase output current/voltage and decrease the matching resistive load. In addition, effect of the load resistance on the voltage, current and active power density is also discussed. Finally, a comparison of various piezoelectric material based power output in MLC-system has been also presented.

**Key words:** Piezoelectrics, multilayer, energy harvesting

## INTRODUCTION

Energy harvesting from wasted/unused power sources is being currently studied by numerous researchers for various applications including industrial and automobile machines, human activity, structures and environmental sources.<sup>1–6</sup> In this direction, energy recovery/conversion from environmental vibration/motion-based systems has attracted great interest.<sup>1,7–10</sup> This is because it can be used for remote/wireless and micro-electro-mechanical systems (MEMS) applications as an alternatives power source.<sup>1,11</sup> In this context, three most

popular ways for mechanical-to-electric energy conversion are (1) piezoelectric, (2) electromagnetic and (3) electrostatic transductions.<sup>7,12–18</sup> Out of these, piezoelectric energy harvesters are commonly used for wireless and MEMS based devices. Therefore, during the last decade, a number of researchers have suggested various designs and methods such as: bimorph, cymbal type, stacked layers, functionally graded material (FGM), piezoelectric active fiber composites (AFCs), flexible piezoelectric polymer composite and multilayer ceramics (MLC), to improve the piezoelectric energy harvesting (PEH) capacity.<sup>19–30</sup> Regardless of these developments, there are still numerous challenges that must be addressed for the wireless application based PEH system. These include low power density, fatigue, a fabrication process and cost effectiveness.<sup>6,23</sup> A

major factor hindering the implementation of PEH in practical applications is low power density. Thus, several types of PEH have low power density due to high matching impedance in spite of their high output voltage.

The electrical energy from the PEH can be extracted in two ways: delivering the generated electrical energy across a resistive load, and storing the energy into a capacitor/battery. However, these are challenging issues for PEH study, which has caused researchers to pay more attention to addressing energy delivery and storage working at resonance modes.<sup>23,31</sup> Recently, several researchers are working to solve this problem.<sup>23,28,31–33</sup> Song et al.<sup>32</sup> fabricated MLC-based PEH which consisted of lower impedance matching and higher current density. However, they only reported directly measured output voltage of the harvester and calculated current and power, which indicates that the reported power is apparent power instead of active power. However, apparent power is not a true indicator of performance for real time applications. Therefore, direct measurement of active power for the MLC-PEH systems and a detailed discussion is necessary. Another important parameter for the PEH is to have a higher transduction coefficient, which can be defined as<sup>34</sup> Transduction coefficient =  $d_{ij} \times g_{ij} = \frac{d_{ij}^2}{\epsilon_{ij}^T}$  where  $d_{ij}$ ,  $g_{ij}$  and  $\epsilon_{ij}^T$  are piezoelectric charge constant, piezoelectric voltage constant and dielectric constant, respectively. For a material to be a good PEH candidate it should have a high piezoelectric constant and low dielectric constant. In our previous study, 0.5CPZT-PZNN ceramics were observed to have a very high transduction coefficient of around 20,367 m<sup>2</sup>/N.<sup>33</sup> Therefore, in the present work, we fabricated multi-layer 0.5CPZT-PZNN ceramics and investigated the PEH characteristic. We also studied the effect of the number of stacked layers. Additionally, a comparison of the power density has been made with other important PEH materials.

## EXPERIMENTAL PROCEDURE

A 0.5 mol.% CuO sample containing 0.69Pb(Zr<sub>0.47</sub>Ti<sub>0.53</sub>)O<sub>3</sub>-0.31Pb(Zn<sub>0.4</sub>Ni<sub>0.6</sub>)<sub>1/3</sub>Nb<sub>2/3</sub>O<sub>3</sub> (0.5CPZT-PZNN) ceramic powder was prepared and *n*-layer stacked MLC harvesters were fabricated. The detailed description of ceramic powder preparation and MLC fabrication were reported in previous work.<sup>33</sup> Figure 1a shows a schematic representation with detailed dimensions of prepared MLC. The phase formation of 0.5CPZT-PZNN ceramics was investigated by x-ray diffraction (XRD: Rigaku D/max-RC, Tokyo, Japan). The microstructures and compositions of the specimens were investigated by scanning electron microscopy (SEM: Hitachi S-4300, Osaka, Japan) and energy-dispersive x-ray spectroscopy (EDX: EMAX, Horiba, Kyoto, Japan). The flat face of the bulk ceramic

sample was ground and a silver electrode was sputtered on both surfaces. Then, the temperature dependent dielectric measurement (HP 4284A; Hewlett Packard Corporation, Palo Alto, CA, USA) was performed from 50°C to 300°C with a heating rate of 5°C/min. The bulk ceramics and MLC layers were poled in silicone oil at 120°C for 60 min under the direct current (DC) field of 3.0 kV/mm. Further, for the fabrication of MLC cantilever harvesters, layers were attached to a steel leaf spring substrate using epoxy (353ND; Epoxy Technology, Billerica, MA, USA) as shown in Fig. 1b. Figure 1b shows the schematic diagram of single layer cantilever (*n* = 1 represent the bulk ceramics). Figure 1c shows the top views and side view of three-layer MLC. In the three-layer MLC, each side, 2 mm in length, is not an electrode to avoid a short circuit; therefore, the length of the electrode is 15 mm and width is 2.9 mm, while the thickness of each electrode layer is ~ 3.2–4 μm. Similarly, electrode configuration is also used for five-layer and seven-layer MLC. External vibration was applied using an artificial exciter (Type 4809; Bruel & Kjaer, Bremen, Germany), and the vibration acceleration was 1.0 *g* (*g* = 9.8 m/s<sup>2</sup>). The output voltage, current and electric power were directly measured using a microwattmeter (HP 5347A; Hewlett Packard Corporation, Palo Alto, CA, USA) at various electric load resistances and external vibration frequencies.

## RESULTS AND DISCUSSION

Figure 2 shows the XRD patterns of 0.5CPZT-PZNN ceramics sintered at 900°C for 4 h. All the XRD peaks are indexed using the JCPDS file no. 86-1712, which is consistent with the literature.<sup>33</sup> It shows homogeneous perovskite phase formation without any secondary phase, indicated by absence of any extra peaks. 0.5CPZT-PZNN ceramics possess a well-known rhombohedral structure with a lattice parameter of *a* = *b* = *c* = 4.045 Å and  $\alpha = 89.8^\circ$ .<sup>33</sup> A detailed discussion on the XRD analysis has been previously reported.<sup>33</sup> Therefore, the present work is limited to confirming the phase formation of the composition under study. It is already established that the 0.5CPZT-PZNN ceramics have a high transduction coefficient (20,367 m<sup>2</sup>/N) at room temperature.<sup>33</sup> Therefore, similar rhombohedral structure is also employed in the present work.

In order to further investigate the material, temperature dependence of dielectric constant and loss were measured. Figure 3a and b displays the dielectric constants ( $\epsilon$ ) and loss versus temperature plot at various frequency (100–100 kHz). Inset of Fig. 3 represents the enlarged view of (1) dielectric constant near room temperature to 200°C, (2) dielectric constant and (3) dielectric loss in the vicinity of Curie temperature (*T*<sub>c</sub>). Dielectric plots suggest normal ferroelectric behavior with one anomaly near *T*<sub>c</sub> of 300°C. This higher *T*<sub>c</sub> is needed

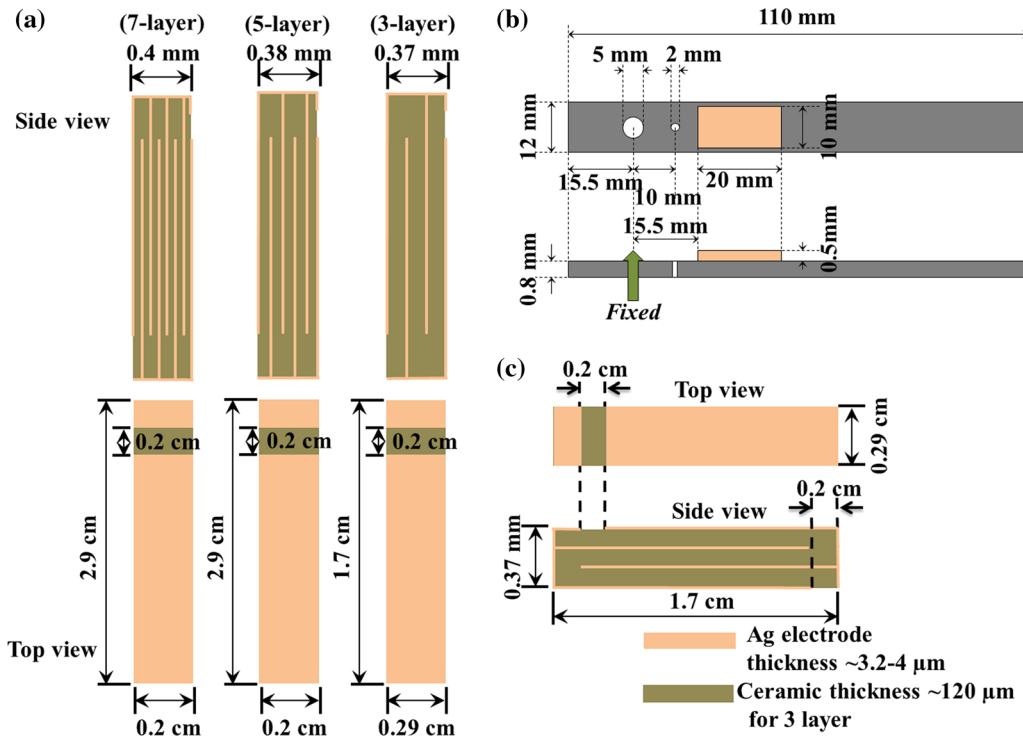


Fig. 1. Schematics for the (a)  $n$ -layers 0.5CPZT-PZNN MLC, (b) cantilever-type bulk piezoelectric harvester and (c) three-layer 0.5CPZT-PZNN MLC.

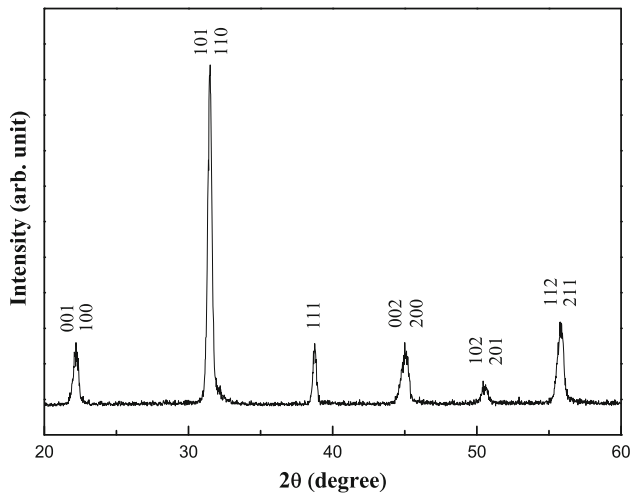


Fig. 2. XRD patterns of sintered 0.5CPZT-PZNN ceramics.

for PEH because when mechanical loss is generated, the temperature of harvester could increase during the real time application. Moreover, 0.5CPZT-PZNN ceramics show low dielectric loss value ( $< 1.0\%$ ). Therefore, 0.5CPZT-PZNN ceramics have an additional advantage pertaining to the PEH system. Further,  $T_c$  shifted towards the higher temperature side with increasing frequency (inset of Fig. 3a) while  $\epsilon$  at  $T_c$  decreased, which is typical behavior of ferroelectric relaxor material.<sup>35</sup> Generally, 0.5CPZT-PZNN consists of mixed ferroelectric phases such as rhombohedral, tetragonal and pseudo-cubic because their solid solution lies

between normal ferroelectric PZT and typical relaxor PZNN.<sup>33</sup> Hence, one can expect that 0.5CPZT-PZNN ceramics have a relaxor-like ferroelectric behavior.

Figure 4a shows the SEM image of the MLC ( $n = 3$ ) 0.5CPZT-PZNN ceramics as-fabricated at  $900^\circ\text{C}$  using a Ag electrode. The enlarged view at the interface of the Ag electrode and 0.5CPZT-PZNN ceramic layer is represented in Fig. 4b. MLC are well-developed with dense micro-structure and the thickness of one layer is approximately  $120\ \mu\text{m}$ , whereas the electrode thickness is  $\sim 3.2\text{--}4\ \mu\text{m}$ . For further investigation of diffusion, EDX line scanning was conducted across the Ag electrode and the 0.5CPZT-PZNN ceramic layers as shown in Fig. 4c. Ag peaks are not observed in the EDX spectrum of the ceramics region. Similarly, Pb, Zr, Ti, Ni and Nb ions spectra are not observed in the Ag electrode region. Hence, it can be said that the diffusion between the Ag electrode and the 0.5CPZT-PZNN ceramic layer has not occurred during fabrication. The SEM and EDX results suggest that MLC have been very well fabricated without any diffusion between electrode and ceramics.

Figure 5 shows the output (a) electric field, (b) current and (c) power density for  $n$ -layer ( $n = 1, 3, 5$  and  $7$ ) MLC harvesters with respect to operating frequency at certain load resistance. All the  $n$ -layer ( $n = 1, 3, 5$  and  $7$ ) harvesters have a similar resonance frequency ( $\sim 80\ \text{Hz}$ ) because the size, shape and Young's modulus of harvesters are the same as reported in experimental procedures. Here,

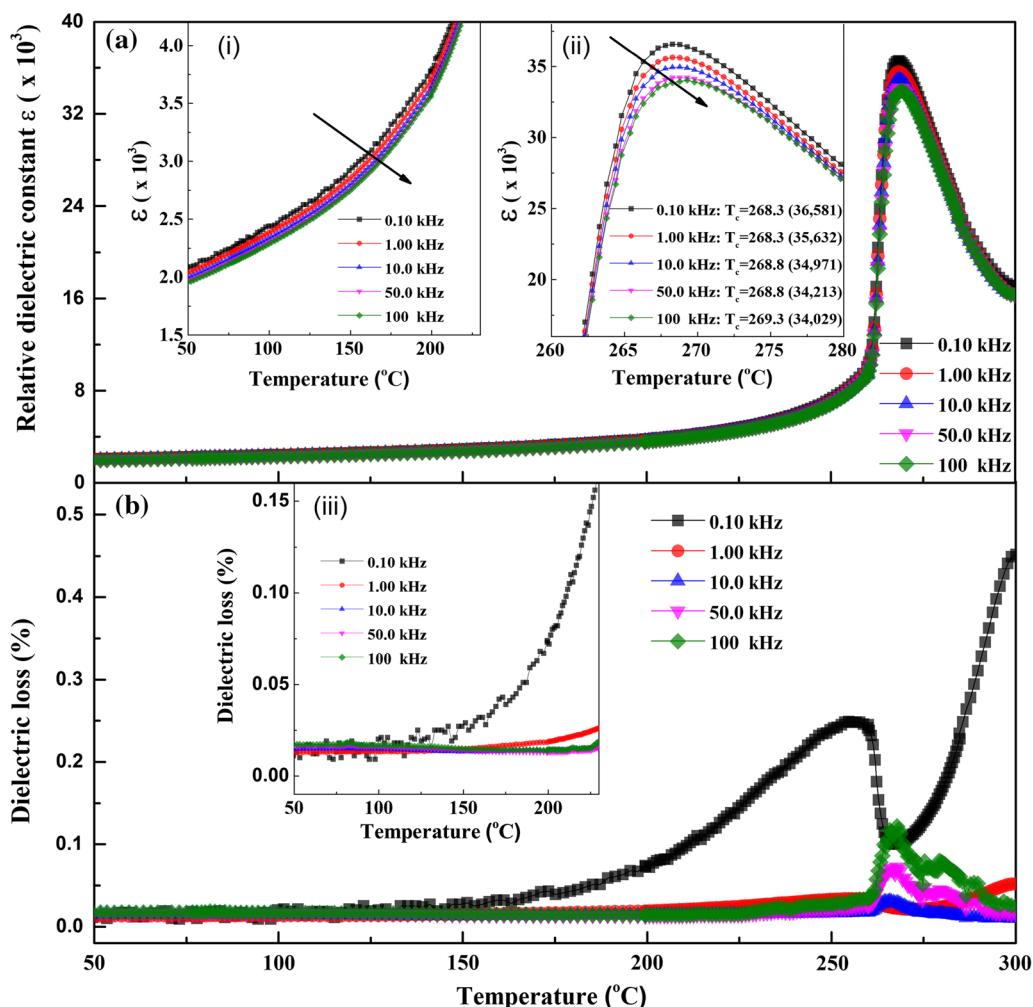


Fig. 3. (a) Dielectric constant and (b) loss versus temperature plots at various frequency for sintered 0.5PZT-PZNN ceramics. Inset shows an enlarged view of (i) dielectric constant near room temperature, (ii) dielectric constant and (iii) dielectric loss behavior in the vicinity of Curie temperature.

it is important to note that the Young's modulus of PEH harvesters are assumed to be the same as steel leaf spring substrate because the multi-layer ceramic has a tiny volume portion as compared to the base layer. Therefore, the Young's modulus of PEHs are independent of the number of layers of multi-layer ceramics. Generally, it is established that in the PEH-system, maximum output electric field, current density and power density can be obtained at the resonance frequency owing to maximum harvester displacement.<sup>1</sup> Hence, it is important to note that cantilevers were designed in such a way that they can operate using an ambient frequency of approximately 80 Hz and can be used for self-powering devices. The bulk harvester ( $n = 1$ ) shows a high electric field with low current density. However, if  $n$  is more than 1 (MLC harvester), the electric field is decreased while the current density is increased with increments in  $n$ . A theoretical model is introduced by Kong et al.<sup>36</sup> to address electrical load matching issues for complex load and/or impedances. However, the theoretical estimated

resistive impedance matching could not become practice and the efficiency drops sharply outside the frequency range. In practice, the trial and error method to find the maximum electrical power delivered across the resistive load for PEH study is commonly used because it has the following advantages: (1) inexpensive, (2) simple and practicable, (3) a maximum power can be obtained with a matched resistive load, and (4) the value obtained is significantly larger than that stored in a super-capacitor/battery.<sup>23,31,36</sup> Therefore, this method is also used in the present work. Hence, to see the effect of load resistance and number of layers, the frequency is fixed at 80 Hz. The output voltage, current and power density of  $n$ -layer MLC ( $n = 1, 3, 5$  and  $7$ ) harvesters has been presented in Fig. 5d, e, and f, respectively, as a function of load resistance corresponding to resonance frequency.

The output electric field increases as the load resistance increases. On the other hand, current densities decrease with increase in load resistance. It can be due to the rise of total resistance in electric

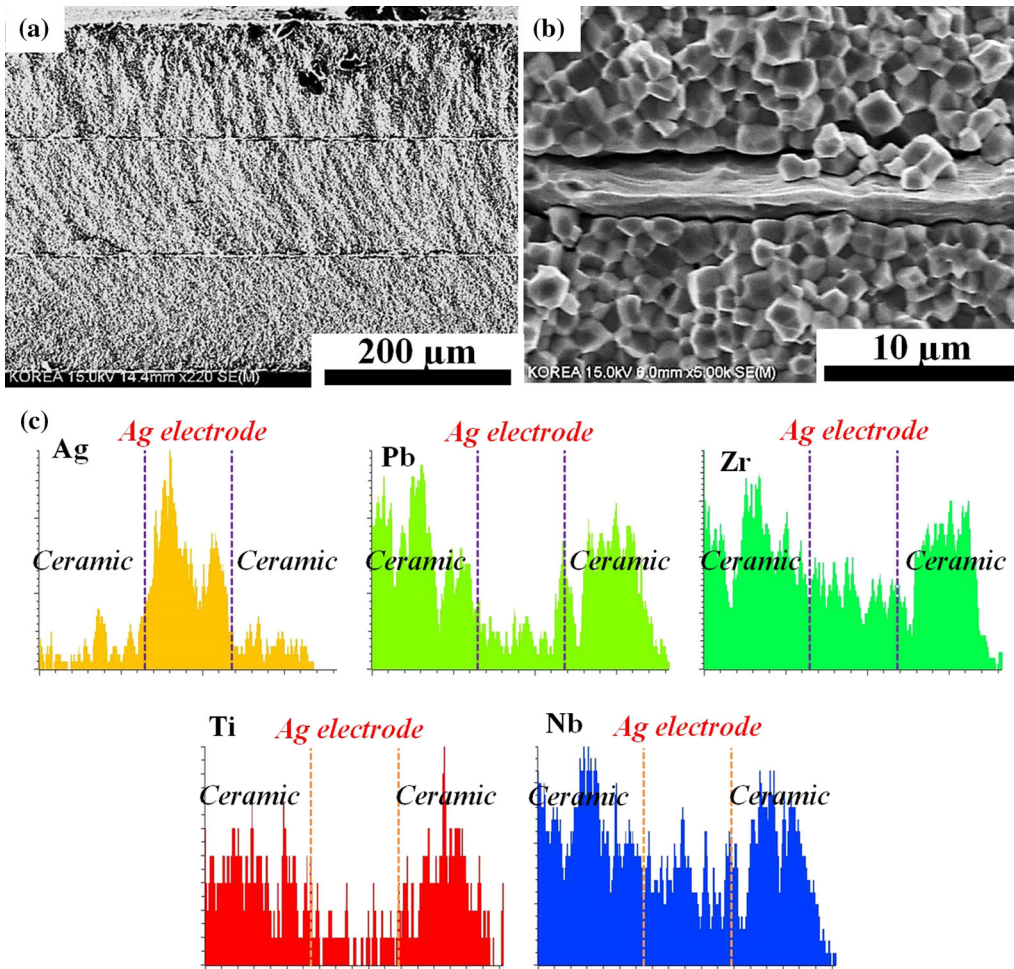


Fig. 4. SEM image of three-layer MLC sample (a) low magnification and (b) high magnification and (c) EDS line scan spectrum of ceramics and Ag electrode.

circuit. In the bulk harvester ( $n = 1$ ) the maximum output power density is obtained as  $21.0 \text{ mW/cm}^3$  across a  $1 \text{ M}\Omega$  load resistance. As the load resistance further increase ( $> 1 \text{ M}\Omega$ ), power density decreases. Therefore, the output power of the piezoelectric harvester strongly depends on the load resistance and it attains maximum values when the load impedance equals the source impedance. As the number of layers increase, the load resistances for impedance matching are dramatically reduced see Fig. 5g. This behavior of MLC can be understood by the impedance matching model as reported by Song et al.<sup>32</sup> The total impedance of the harvester is decreased with increment of capacitor value as  $R = \frac{1}{2\pi \times f \times C}$  where  $R$ ,  $f$  and  $C$  are total impedance, frequency and capacitance of piezoelectric material, respectively. In MLC, capacitance is proportional to number of stacked layers,  $n$ . Therefore, the total impedance of MLC harvesters is much smaller than that of a bulk harvester. Hence, the maximum output power density can be obtained at lower values of load resistance. Additionally, this low impedance matching affects the small electric field

output and high current density because total resistance of the whole circuit is reduced, as depicted in Fig. 5h and i, respectively. Figure 5g, h, i, and j shows the matching impedance, electric field, current density and maximum power density of  $n$ -layer MLC harvesters with respect to the number of stacked layers ( $n$ ), respectively. As  $n$  increases, the matching impedance of MLC harvesters continuously decreases. Hence, the electric field decreases while the current density increases with increment in  $n$ . Therefore, MLC harvesters have better performance as compared to bulk harvesters.

Furthermore, the output power density of MLC harvesters is independent of the number of stacked layers and displays lower matching impedance, which results in higher current density.<sup>32</sup> However, the present work shows that the output power densities of MLC harvesters are also enhanced with increment in  $n$ , even though products of output electric field and current density of all the samples are similar. This could be explained by the active and reactive power of the piezoelectric harvester. In

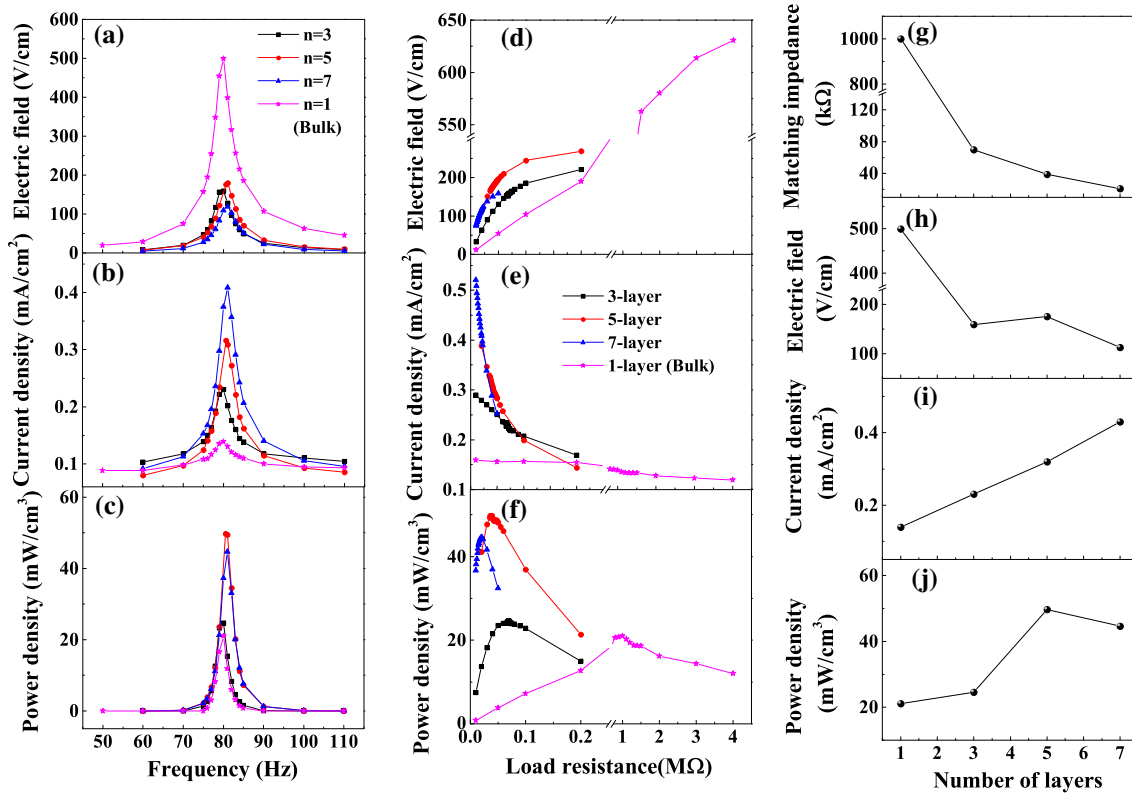


Fig. 5. The output (a) electric field, (b) current density and (c) power density versus operating frequency of  $n$ -layer MLC (at each matching impedance). The output (d) electric field, (e) current density and (f) power density as a function of load resistance at each resonant frequency for  $n$ -layer MLC. The (g) matching impedance, output (h) electric field, (i) current density and (j) power density with respect to the number of stacked layers.

general, the apparent power is known as the production of output voltage and current, and it consists of active and reactive power.<sup>37</sup> In the case of an alternative power source, the circuit has a reactance factor which is same as inductor. This makes the phase difference between voltage and current. As a result, some part of current (Sign term of current) is orthogonal with the voltage and this part cannot contribute to work on the load resistance.<sup>37</sup> This un-contributed work means reactive power. Therefore, only active power must be considered an exact electric power generated by the piezoelectric harvester. The bulk piezoelectric harvester shows large impedance, which means that it has a large reactance. Thus, their active power is very low even though their apparent power is the same as MLC harvesters. In this case, MLC harvesters have small impedance due to their high capacitance. Hence, their reactance could be suppressed and their active power could be enhanced by increasing the number of layers. Therefore, MLC harvesters show not only high current density, but also a large amount of output power density as compared to bulk harvesters. However, as  $n$  is increased beyond five, the active power density slightly decreases. For a seven-layer stacked MLC, the capacitance is very high as compared to others. When the capacitance of MLC is too high, internally stored energy in MLC varies as  $E = \frac{1}{2}CV^2$ . In this

case, generated electric energy is almost consumed inside the ceramics and the active power density is decreased. Therefore, the maximum output power density of 49.7 mW/cm<sup>3</sup> with low matching impedance (39 kΩ), low electric field (175.4 V/cm) and high current density (0.32 mA/cm<sup>2</sup>) is obtained when  $n$  is 5. The measured capacitance of three-layer MLC is  $\sim 0.5$  nF/mm<sup>3</sup>. From this value, the capacitance of each MLC-PEH can be calculated. The capacitance for a single layer ( $C_S$ ) and multi-layer ( $C_M$ ) is defined as<sup>23,31,38</sup>

$$C_S = \epsilon_r \epsilon_0 \frac{A}{t_S} \text{ and } C_M = \epsilon_r \epsilon_0 n \frac{A}{t_M} = \epsilon_r \epsilon_0 n^2 \frac{A}{L} \quad (1)$$

where  $\epsilon_0$  and  $\epsilon_r$  are the permittivity of vacuum and relative permittivity of the piezoelectric material,  $A$  is the electrode area of the single layer,  $t_S$  is the thickness of the single layer,  $t_M$  is the thickness of each layer in MLC, which is equal to the  $t_S$ ,  $L(L = nt_M)$  is the total thickness on the MLC piezoelectric layer. This shows that the  $C_M$  is  $n^2$  times the  $C_S$  for the same overall size; the MLC has high energy storage capability. However,  $n^2$  times  $C_S$  relation isn't applicable for the current work as the thickness of the MLC layer is different in each case. The present work focused on keeping resonance frequency ( $\sim 80$  Hz) the same, hence total volume (size, shape) stayed constant instead of the

**Table I. Energy harvesting characters of several reported MLC harvesters**

Power (mW)	Dimensions (cm)			Frequency (Hz)	Force (g)	Power density (mW/cm <sup>3</sup> )	References
	<i>l</i>	<i>w</i>	<i>h</i>				
100	3.5	1.0	0.02	143	240		Ref. 32
0.903	3.5	0.7	0.032	20	0.43	15.5	Ref. 28
0.347	3.04	0.7	0.7	1204	2258		Ref. 23
39	–	2.9Ø	0.1	100	795	60	Ref. 21*
0.083	2.2	2.3	0.015	64.2	0.29		Ref. 41
1.1	2.9	0.2	0.038	80	1	49.7	This work

\*Symbol type.

layer thickness. The capacitance values of bulk PEH, three-layer, five-layer and seven-layer MLC-PEHs are  $\sim 0.6$  nF,  $\sim 9$  nF,  $\sim 25$  nF and  $\sim 50$  nF, respectively. However, the capacitance is also estimated by an AC-component exhibiting reactance equation as  $C = 1/(2\pi \times f \times R)$ , which is found as  $\sim 2$  nF,  $\sim 28$  nF,  $\sim 51$  nF,  $\sim 95$  nF for of bulk PEH, three-layer, five-layer and seven-layer MLC-PEHs, respectively. In addition, the capacitance of bulk and three-layer MLC is calculated by the electrode size and dielectric constant as  $\sim 2.7$  nF and  $\sim 14$  nF, which is comparable to the directly measured capacitance. The detailed discussion on these measurement method are discussed by Jonassen<sup>39</sup> Generally, the powers of 0.9 mW and 0.09 mW are necessary for operating and deep sleep state for commercial RF transceiver, respectively. Therefore, using one MLC-PEH device in this paper, at least one RF transceiver can be operated, which means that MLC-PEH device are very suitable for a micropower source of a ubiquitous sensor network.

Finally, Table I lists the energy harvesting characteristics comparison of various piezoelectric MLC with their operating parameters and dimensions.<sup>23,28,29,40</sup> The direct comparison of energy harvesting character is difficult because each harvester is operated under different conditions: such as operating mode, force and frequency. Nevertheless, the output power in this work shows the remarkable value. Moreover, our energy harvester has high output current density as well as power density, as discussed. This is because of as increasing the number of layers, total impedance of PEH are decreases which leads to high output current density. Therefore, it can be considered that MLC harvesters using 0.5CPZT-PZNN ceramics are suitable candidates for future power source of sensor network, wireless and self-powering devices.

## CONCLUSIONS

Energy harvesting potential of CuO added 0.69Pb(Zr<sub>0.47</sub>Ti<sub>0.53</sub>)O<sub>3</sub>-0.31Pb(Zn<sub>0.4</sub>Ni<sub>0.6</sub>)<sub>1/3</sub>Nb<sub>2/3</sub>O<sub>3</sub> (0.5CPZT-PZNN)-based multi-layer ceramics (MLC) was investigated. The *n*-layer (*n* = 1, 3, 5 and 7) MLC were successfully fabricated without any diffusion between ceramic layer and Ag electrode. In the bulk ceramic (*n* = 1), the energy harvester matches the impedance with high load resistance, which displayed a very high output electric field of 499.2 V/cm and low current density of 0.14 mA/m<sup>2</sup>. However, in the case of MLC, the opposite behavior is observed due to increase in capacitances with increasing number of stacked layer *n*. Thus, the matching impedance and output electric field were decreased while output current density was increased with respect to *n*. Especially, the output power densities of MLC harvesters also increased with increasing *n* even though production of electric fields and current densities of all specimens were similar. This behavior might be related to active electric power. However, when *n* = 7, this active power density was decreased due to the higher capacitance. Therefore, five-layer 0.5CPZT-PZNN MLC harvesters exhibited a high output power density of 49.7 mW/cm<sup>3</sup> at 80.6 Hz with a high output current density of 0.32 mA/cm<sup>2</sup>. The results indicate that the proposed approach can be a good candidate for power source of wireless and MEMS-based electric devices. The results show the potential of PEH for use in power harvesting applications and estimating the amount of energy stored in capacitor with time required to recharge a specific capacity battery.

## ACKNOWLEDGMENTS

In-Tae Seo and Satyanarayan Patel acknowledge financial support under the Alexander von Humboldt Fellowship.

### CONFLICT OF INTEREST

The author(s) declared no potential conflict of interest with respect to the research, authorship, and/or publication of this article.

### REFERENCES

1. S. Priya and D.J. Inman, *Energy Harvesting Technologies* (New York: Springer, 2009).
2. J.A. Paradiso and T. Starner, *IEEE Pervasive Comput.* 4, 18 (2005).
3. P.D. Mitcheson, E.M. Yeatman, G.K. Rao, A.S. Holmes, and T.C. Green, *Proc. IEEE* 96, 1457 (2008).
4. S.-G. Kim, S. Priya, and I. Kanno, *MRS Bull.* 37, 1039 (2012).
5. L. Mateu, M. Echeto, and F. De Borja, Review of energy harvesting techniques and applications for microelectronics, in *VLSI Circuits and Systems II, SPIE the International Society for Optical Engineering*, vol. 5837 (2005), pp. 359–373.
6. S. Priya, *J. Electroceram.* 19, 167 (2007).
7. H. Li, C. Tian, and Z.D. Deng, *Appl. Phys. Rev.* 1, 041301 (2014).
8. H. Kulah and K. Najafi, An electromagnetic micro power generator for low-frequency environmental vibrations, in *17th IEEE International Conference on Micro Electro Mechanical Systems. Maastricht MEMS 2004 Technical Digest*, (IEEE, 2004) pp. 237–240.
9. S. Roundy, E.S. Leland, J. Baker, E. Carleton, E. Reilly, E. Lai, B. Otis, J.M. Rabaey, P.K. Wright, and V. Sundararajan, *IEEE Pervasive Comput.* 4, 28 (2005).
10. S. Meninger, J.O. Mur-Miranda, R. Amirtharajah, A. Chandrakasan, and J.H. Lang, *IEEE Trans. VLSI Syst.* 9, 64 (2001).
11. K.A. Cook-Chennault, N. Thambi, and A.M. Sastry, *Smart Mater. Struct.* 17, 043001 (2008).
12. F.U. Khan, *J. Renew. Sustain. Ener.* 8, 044702 (2016).
13. K.Q. Fan, B. Yu, Y.M. Zhu, Z.H. Liu, and L.S. Wang, *Int. J. Mod. Phys. B* 31, 1741011 (2017).
14. F.U. Khan and Izhar, *Sadhana Acad. Proc. Eng. Sci.* 41, 397 (2016).
15. C.G. Cooley, *Mech. Syst. Signal Process.* 94, 237 (2017).
16. Y.L. Zhang, T.Y. Wang, A. Zhang, Z.T. Peng, D. Luo, R. Chen, and F. Wang, *Rev. Sci. Instrum.* 87, 125001 (2016).
17. M. Lallart, S. Pruvost, and D. Guyomar, *Phys. Lett. A* 375, 3921 (2011).
18. A.C.M. De Queiroz, *Analog Integr. Circuits Signal Process.* 85, 57 (2015).
19. Y.T. Hu, T. Hu, and Q. Jiang, *Acta Mech. Solida Sin.* 20, 296 (2007).
20. A. Erturk and D.J. Inman, *Smart Mater. Struct.* 18, 025009 (2009).
21. H.W. Kim, A. Batra, S. Priya, K. Uchino, D. Markley, R.E. Newnham, and H.F. Hofmann, *Jpn. J. Appl. Phys.* 1, 6178 (2004).
22. J. Palosaari, M. Leinonen, J. Hannu, J. Juuti, and H. Jantunen, *J. Electroceram.* 28, 214 (2012).
23. T.-B. Xu, E.J. Siochi, J.H. Kang, L. Zuo, W. Zhou, X. Tang, and X. Jiang, *Smart Mater. Struct.* 22, 065015 (2013).
24. S.L. Vatanabe, G.H. Paulino, and E.C.N. Silva, *Comput. Methods Appl. Mech. Eng.* 266, 205 (2013).
25. Y. Shi, H. Yao, and Y.W. Gao, *J. Alloy. Compd.* 693, 989 (2017).
26. Z.T. Yang, D.P. Zeng, H. Wang, C.L. Zhao, and J.W. Tan, *Smart Mater. Struct.* 24, 075029 (2015).
27. Y. Yang, L. Tang, and H. Li, *Smart Mater. Struct.* 18, 115025 (2009).
28. Y. Yan, A. Marin, Y. Zhou, and S. Priya, *Energy Harvest. Syst.* 1, 189 (2014).
29. S.-J. Jeong, M.-S. Kim, J.-S. Song, and H.-K. Lee, *Sensors Actuators A: Phys.* 148, 158 (2008).
30. H.S. Kim, J.-H. Kim, and J. Kim, *Int. J. Precis. Eng. Manuf.* 12, 1129 (2011).
31. T.-B. Xu, E.J. Siochi, J.H. Kang, L. Zuo, W. Zhou, X. Tang, and X. Jiang, in *A Piezoelectric PZT Ceramic Multilayer Stack for Energy Harvesting Under Dynamic Forces* (American Society of Mechanical Engineers, 2011), p. 1193.
32. H.-C. Song, H.-C. Kim, C.-Y. Kang, H.-J. Kim, S.-J. Yoon, and D.-Y. Jeong, *J. Electroceram.* 23, 301 (2009).
33. I.T. Seo, T.G. Lee, D.H. Kim, J. Hur, J.H. Kim, S. Nahm, J. Ryu, and B.Y. Choi, *Sensors Actuators A: Phys.* 238, 71 (2016).
34. I.T. Seo, Y.J. Cha, I.Y. Kang, J.H. Choi, S. Nahm, T.H. Seung, and J.H. Paik, *J. Am. Ceram. Soc.* 94, 3629 (2011).
35. C.J. Stringer, T.R. Shrout, and C.A. Randall, *J. Appl. Phys.* 101, 054107 (2007).
36. N. Kong, D.S. Ha, A. Erturk, and D.J. Inman, *J. Intell. Mater. Syst. Struct.* 21, 1293 (2010).
37. H. Edelmann, *Siemens Forsch Entwickl.* 10, 16 (1980).
38. M. Jabbari, M. Ghayour, and H.R. Mirdamadi, *J. Eng. Mater. Technol.* 139, 031008 (2017).
39. N. Jonassen, Human body capacitance: static or dynamic concept?[ESD], in *Electrical Overstress/Electrostatic Discharge Symposium Proceedings (Cat. No. 98TH8347)* (IEEE, 1998), p. 111.
40. H. Kim, S. Priya, H. Stephanou, K. Uchino, and I.E.E.E. Trans, *Ultrason. Ferroelectr. Freq. Control* 54, 1851 (2007).
41. D. Zhu, A. Almusallam, S. Beeby, J. Tudor, and N. Harris, in *A bimorph multi-layer piezoelectric vibration energy harvester* (Power MEMS, Belgium, 2010).

**Publisher's Note** Springer Nature remains neutral with regard to jurisdictional claims in published maps and institutional affiliations.